

EROS/MACHO Gravitational Microlensing Events Toward LMC in Evans Halo Model

Sohrab Rahvar*

Department of Physics, Sharif University of Technology,

P.O.Box 11365–9161, Tehran, Iran

Institute for Studies in Theoretical Physics and Mathematics,

P.O.Box 19395–5531, Tehran, Iran

December 2, 2024

Abstract

After one decade from gravitational microlensing experiments, 13 to 17 event by MACHO (depends of quality) and two event by EROS have been detected toward Large Magellanic Cloud. We use Evans spherically symmetric halo models to study the rate of microlensing events in this direction. The expected number of events obtain by applying the experimental observational efficiency of EROS and MACHO in galactic models. We then compare those numbers with the observed events to obtain the fraction of halo that is made by Machos. It is shown that results derived from two experiments are in good agreement with each other and except the minimal halo model, Machos comprise only a fraction (depending on the model) of Milky Way halo. The results are also compatible with White Dwarfs population studies in the Hubble Deep Field.

1 Introduction

The existence of dark matter is evidence by studying the rotational curve of spiral galaxies [1] & [2]. Recent results of optical and 21 cm bands observation shows that for the thousand of spiral galaxies, the Keplerian rotational velocity beyond the luminous radius remains constant [3]. X ray diffusion emission in elliptical galaxies and dynamics of cluster of galaxies also shows that there should be a halo structure for the spiral galaxies. Various dark matter candidates have been proposed until now, like baryonic dark matter and exotic dark matters like Axions, massive neutrinos, WIMPs and Super-symmetric particles. However, simulations shows that there is a discrepancy between expected rotational velocity due to cold dark matter of halo and observed velocity curves [4] & [5].

In the case of baryonic dark matter, Big Bang nucleosynthesis models gives $\Omega_B h^2 = 0.02$ [6] & [7] while measuring the mass of luminous stars obtain Ω_{lum} of universe about 0.004 [8]. Comparing Ω_B with Ω_{lum} ($\Omega_B \gg \Omega_{lum}$), gives an other evidence

*E-mail:rahvar@mehr.sharif.edu

for the existence of baryonic dark matter. One of the types of baryonic dark matter could be in the form of Massive Astrophysical Compact Halo Objects (Macho). These objects due to their light masses are obscure. Neutron stars and black holes as dark objects also can be considered in this category. The pioneer work of using gravitational microlensing technique for detection of Macho was proposed by Paczyński [9]. Since his proposal, microlensing searches have turned very quickly into reality and some groups like AGAPE, DUO, EROS, MACHO, OGLE and PLANET have started to do this experiment. During this decade, the final results of experiments compared with the theoretical expected results to put a constraint on the fraction of halo that is made by Macho objects. It is clear that the conclusion about the contribution of Machos in dark matter strongly depends on galactic halo model and mass function of Machos. Using standard model for Milky Way and delta mass function for Machos, EROS and MACHO groups could obtain the fraction of halo that is made by Machos. EROS collaboration put a strong constraint on the fraction of halo made of objects in the range $[10^{-7} M_{\odot}, 4M_{\odot}]$, excluding at 95% C.L. that more than 40% of the standard halo is made of objects with up to one solar mass [11]. The analysis of 5.5 yrs of LMC observations by the MACHO group also estimate that the halo mass fraction in the form of compact halo objects is about 20% [12].

Here in this work, we use the most general spherically symmetric model for the halo of spiral galaxies that interpret Keplerian rotational curves[10]. The expected distribution of gravitational microlensing events obtain by applying the efficiency of EROS and MACHO experiments in these models. Here we use power law mass function for the compact halo objects and HST observed mass function for the galactic disk. We compare the expected rate of events with those have been observed experimentally to evaluate the fraction of halo made by machos.

The organization of paper is as follows. In Sect. 2, we introduce the basics of gravitational microlensing and obtain relation between the optical depth and the rate of microlensing events. In Sect. 3 we introduce Evans model for galactic structure and in Sect. 4 we obtain the expected rate of microlensing events for six different galactic models toward LMC by using Monte-Carlo simulation. We then calculate the fraction of halo made by Macho in different galactic halo. The results are discussed in Sect. 5.

2 Basics of gravitational microlensing

In this section we present the main feature of gravitational microlensing and in particular, we obtain relation between optical depth and the rate of events. For review see ([13], [14], [15], & [16]).

According to general relativistic results, a given light ray bends near a massive star. A considerable gravitational lensing occurs when the line of sight between us and a background star pass enough near a lens. Since the deflection angle in the case of microlensing is too small (taking into account resolution of present apparatus), it is impossible to distinguish two images that are produced due to the gravitational lensing, thus the effect is only on the brightness magnification of background star. This magnification is given by

$$A(t) = \frac{u(t)^2 + 2}{u(t)\sqrt{u(t)^2 + 4}}, \quad (1)$$

where $u(t)^2 = u_0^2 + \left(\frac{t-t_0}{t_E}\right)^2$ is the impact parameter, normalized to Einstein Radius which is defined by

$$R_E^2 = \frac{4GM D_{os}}{c^2} x(1-x). \quad (2)$$

In the definition of Einstein radius, D_{ol} and D_{os} are the distance of the lens and source from the observer and $x = \frac{D_{ol}}{D_{os}}$. Definition of an event is given by constraint on maximum magnification with $A_{max} > 1.34$ or in other word $u < R_E$.

The optical depth and its relation with the rate of events is used in statistical studies of microlensing events. Taking a snapshot from the background stars, the probability of existence the projected background stars inside Einstein Radius of lenses in the lens plane along our line of sight is the definition of optical depth. The optical depth of Machos in the range of $[M, M + dM]$ can be obtain by:

$$d\tau(x; M, M + dM) = \frac{\pi R_E^2}{A} \left(\frac{\rho(x; M, M + dM)}{M} \right) \times (A \cdot dx). \quad (3)$$

$$d\tau(x; M, M + dM) = \frac{4\pi GM}{c^2} D_{os}^2 x(1-x) n(x) g(M) dM dx, \quad (4)$$

where, $\frac{\rho(x; M, M + dM)}{M}$ is the number density of lenses in the range of $[M, M + dM]$ and can be written in terms of total number density and mass function of Macho as follows: $dn(M, M + dM) = n_{total} g(M) dM$. The mass function consider to be normalized to one. We use for a given galactic model, an arbitrary Macho contribution for halo to obtain optical depth. It is seen in Eq.(4) that optical depth is independent from mass of Macho and it depends only on the density distribution of matter. Another quantity that relates to optical depth is the observable rate of events per year per the number background stars and is denoted by Γ .

The expected number of events in the range of $[M, M + dM]$ obtain as follows:

$$dN_{exp}(x; M, M + dM) = \left(\frac{2R_E(x) \langle v_t(x) \rangle T_{obs}}{A(x)} \right) \times (n(x) g(M) dM \times A \cdot dx) \times N_{bg}, \quad (5)$$

where, T_{obs} and N_{bg} are the monitoring time and the number of background stars, $T_{obs} \times N_{bg}$ is called the exposure time. $\langle v_t(x) \rangle$, is the mean transverse velocity of lenses with respect to the line of sight and obtain by velocity distribution function $f_v(x)$ as follows:

$$\langle v_t \rangle = \int v_t(x) f_v(x) d^3 v, \quad (6)$$

where, the distribution function of velocity is normalized to one. The first term in the right hand side of Eq.(5) represents the ratio of spanned tube by a Macho to the projection of background stars zone on the deflector plane, call it $A(x)$. The Second term denotes the number of lenses inside x and $x + dx$ and the last term shows the number of background stars. By definition of $d\Gamma = \frac{dN_{exp}(x)}{N_{bg} T_{obs}}$ and using Eq.(6), the rate of events can be given as follows:

$$d\Gamma(x; M, M + dM) = 2(n(x) g(M) dM) R_E(x)^2 dx \int \frac{v_t(x) \epsilon(t_E)}{R_E(x)} f_v(x) d^3 v \quad (7)$$

where, $\epsilon(t_E)$ is the efficiency of observation and in general case it could depend on all the parameters of microlensing event. We simplify this dependence by averaging over the u_0 , t_0 and stellar magnitude to obtain the efficiency as a function of Einstein crossing time. By substituting Eq.(4) in Eq.(7) and using the definition of Einstein

crossing time $t_E = \frac{R_E}{v_t}$, relation between the rate of microlensing and optical depth can be obtain as follows:

$$d\Gamma(x) = \frac{2}{\pi} d\tau \int \frac{f(x, v)\epsilon(t_E)}{t_E(x, v)} d^3v \quad (8)$$

In the right hand side of Eq.(8), the value of integral is equal to the mean value of $\epsilon(t_E)/t_E$ (the distribution of $f_x(v)$ is normalized to one). Rewriting Eq.(8) yields:

$$d\Gamma(x) = \frac{2}{\pi} d\tau(x) \left\langle \frac{\epsilon(t_E)}{t_E(x)} \right\rangle. \quad (9)$$

We take integral with respect to x , relation between rate of events and optical depth obtain as follows:

$$\Gamma = \frac{2}{\pi} \tau \left\langle \frac{\epsilon}{t_E} \right\rangle. \quad (10)$$

The distribution of expected rate of microlensing events can be obtained by a Monte-Carlo simulation base on using the efficiency of observation and the theoretical rate of events ($\frac{d\Gamma}{dt_E}$). For a given galactic model the theoretical rate of microlensing events, obtain by considering geometrical distribution of matter, velocity distribution and the mass function of lenses of the model. The observational efficiency also is given as a function of event duration, depending on experimental setup. One can use these two distributions to obtain the total expected number of microlensing events as follows:

$$\Gamma = \int \frac{d\Gamma}{dt_E} \epsilon(t_E) dt_E \quad (11)$$

In the next section we introduce different galactic models to obtain the expected rate and the total number of microlensing events toward Large Magellanic Cloud.

3 Galactic models

As we mentioned in the last section, to calculate the rate of events, it needs to know three parameters of galactic model, contained the density distribution, velocity distribution and mass function of lenses. According to classification of galactic structure into three different part of bulge, disk and halo, our aim is to obtain the contribution of each elements in the optical depth and the rate of events toward the our line of sight (Large Magellanic Cloud). Since the contribution of bulge on optical depth toward LMC is negligible, we ignore it in our calculation. In what follows we introduce structure of disk and halo.

3.1 Galactic disk

The density profile of Galactic disk can be given by a double exponential in cylindrical galactic coordinate system (R, z) as follows [17]:

$$\rho(R, z) = \frac{\Sigma_\odot}{2h} \exp \left[-\frac{R - R_\odot}{R_d} \right] \exp \left[-\frac{|z|}{h} \right] \quad (12)$$

where $R_d \sim 3.5 kpc$ is in the order of disk radius and h and Σ_\odot represent the thickness and column density of disk respectively. In our analysis we consider two type of disk which are called thin and thick disk models. The thin disk mainly is made by the population of stars and gas. The column density and thickness of disk in this

model near the sun is about $\Sigma_{\odot} \sim 50 M_{\odot} pc^{-2}$ and $h = 0.32 kpc$. In the case of thick disk, dark matter contribution also is taken into account. In this case, we choose $\Sigma_{\odot} \sim 100 M_{\odot} pc^{-2}$ and $h = 1 kpc$. The rotational velocity of disk also is given by [17]:

$$V_{disk}(R)^2 = 4\pi G \Sigma_{\odot} R_d e^{R_{\odot}/R_d} y^2 [I_0(y)K_0(y) - I_1(y)K_1(y)], \quad (13)$$

where $y = R/(2R_d)$, I_n and K_n are the modified Bessel functions. The velocity distribution for two models of disk is shown in Figure(1).

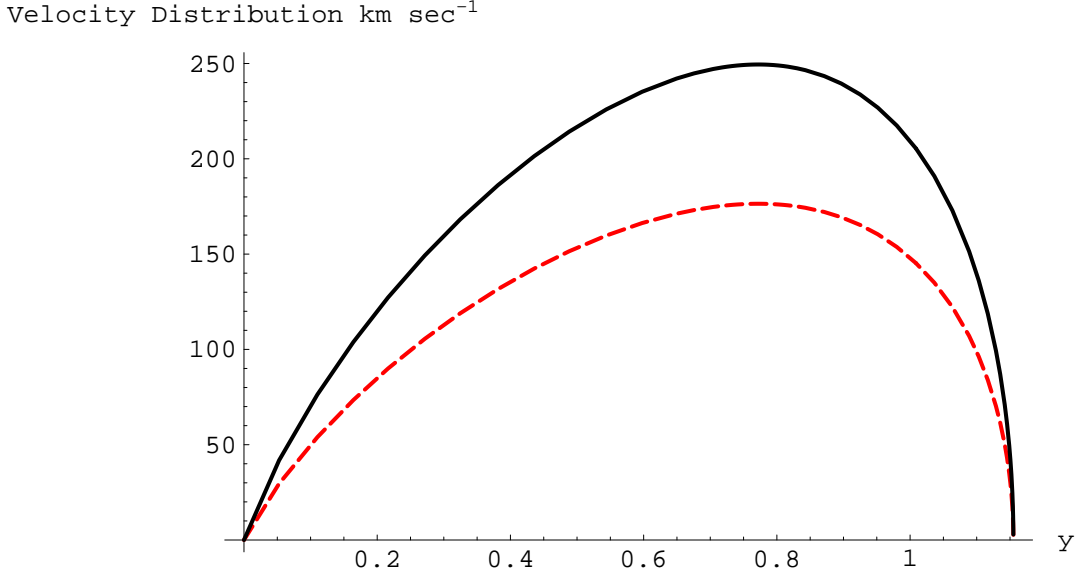


Figure 1: Thick line represents the rotational velocity of thick disk and the dashed line shows this distribution for thin disk. x-axis indicate the distance of disk from the center of galaxy in the term of $y = 2R/R_d$.

3.2 Power law halo model

The largest known set of axisymmetric models with simple distribution functions are called the "power law galaxies". The density of halo in this model is given by:

$$\rho(R, z) = \frac{V_a^2 R_c^{\beta}}{4\pi G q^2} \times \frac{R_c^2(1+2q^2) + R^2(1-\beta q^2) + z^2[2 - (1+\beta)/q^2]}{(R_c^2 + R^2 + z^2/q^2)^{(\beta+4)/2}}, \quad (14)$$

where $R^2 = r^2 + z^2$, R_c is the core radius. q is the flattening parameter, which is the axis ratio of concentric equipotential. $q = 1$ represents a spherical (E0) halo and $q \sim 0.7$ gives an ellipticity of about E6. The parameter of β determines whether the rotational curve asymptotically rises, falls or is flat. At large distance R in the equatorial plane, the rotational velocity can be given by $V_{circ} \sim R^{-\beta}$. So $\beta = 0$ corresponds to flat rotational curve, $\beta < 0$ is a rising rotational curve and $\beta > 0$ is falling. The parameter V_a determines the overall depth of the potential well and hence gives the typical velocities of lenses in the halo. In the spherical symmetric

Evans models ($q = 1$) by coordinate transformation from the center of galaxy to the location of an observer at the position of sun and source stars at the Large Magellanic Cloud ($l=280$, $b=-33$), equation (14) can be obtained by:

$$\rho(r) = \frac{V_a^2 R_c^\beta}{4\pi G} \times \frac{3R_c^2 + (1-\beta)[R_0^2 + r^2 - 2rR_0 \cos(l) \cos(b)]}{[R_c^2 + (1-\beta)(R_0^2 + r^2 - 2rR_0 \cos(l) \cos(b))]^{(\beta+4)/2}}. \quad (15)$$

The velocity dispersion of lenses also is given for different halo models in cylindrical coordinate system as follows [10]:

$$\begin{aligned} \sigma_r^2 &= \sigma_z^2 = \frac{V_a^2 R_c^\beta}{2(1+\beta)} \frac{1}{(R_c^2 + R^2 + z^2/q^2)^{\beta/2}} \\ &\times \frac{2q^2 R_c^\beta + (1-\beta)q^2 R^2 + z^2[2 - (1+\beta)/q^2]}{R_c^2(1+2q^2) + R^2(1-\beta q^2) + z^2[2 - (1+\beta)/q^2]}, \end{aligned} \quad (16)$$

$$\begin{aligned} \sigma_\phi^2 &= \frac{V_a^2 R_c^\beta}{2(1+\beta)} \frac{1}{(R_c^2 + R^2 + z^2/q^2)^{\beta/2}} \\ &\times \frac{2q^2 R_c^\beta + [2 + 2\beta - (1+3\beta)q^2]R^2 + z^2[2 - (1+\beta)/q^2]}{R_c^2(1+2q^2) + R^2(1-\beta q^2) + z^2[2 - (1+\beta)/q^2]}. \end{aligned} \quad (17)$$

In the spherical symmetric Evans models ($q = 1$) for an observer that located at the center of galaxy, it is assumed that velocity distribution in all directions is isotropic. Here we use coordinate transformation from the center of galaxy to obtain velocity distribution for an observer at the position of sun in the direction of Large Magellanic Cloud ($r=52$ kpc, $l=280$, $b=-33$). In the lens plane the transverse velocity distribution is given by taking integral along the line of sight as follows:

$$f(v)v dv = \frac{1}{\sigma^2} \exp\left(-\frac{v^2}{2\sigma^2}\right) v dv, \quad (18)$$

where

$$\begin{aligned} \sigma^2 &= \frac{V_a^2 R_c^\beta}{2(1+\beta)} \frac{1}{[R_c^2 + (1-\beta)(R_0^2 + r^2 - 2rR_0 \cos(l) \cos(b))]^{\beta/2}} \\ &\times \frac{2R_c^\beta + (1-\beta)(R_0^2 + r^2 - 2rR_0 \cos(l) \cos(b))}{3R_c^2 + (1-\beta)(R_0^2 + r^2 - 2rR_0 \cos(l) \cos(b))}. \end{aligned} \quad (19)$$

Here in our study, six galactic models ([18], [19] & [20]) are taking into account with the following parameters:

Model 1a: standard halo and thin disk.

Model 1b: standard halo and thick disk.

Model 2a: power law model ($q=1$ and $\beta = 0$) and thin disk.

Model 2b: power law model ($q=1$ and $\beta = 0$) and thick disk.

Model 4: spherical halo with asymptotic decreasing rotational velocity ($q=1$ and $\beta = 0.2$) and thin disk.

Model 6: spherical halo with flat rotational curve ($q=1$ and $\beta = 0$) and intermediate disk.

Table (1) shows the parameters of these models.

For the standard halo model (1a, 1b), the velocity dispersion of lenses in the halo is independent from space and its value considered about $\sigma = 156 \text{ km/sec}$, While it is seen that for other models, the velocity dispersion depends on the distance of the lens from the observer. Figure (2) shows the transverse velocity distribution of spherically symmetric models 2a, 2b, 4 and 6. Next section contain microlensing Monte-Carlo simulation to evaluate the expected rate of events.

Model :	1a	1b	2a	2b	4	6
$\Sigma_0(M_\odot/pc^2)$	50	100	50	100	50	80
$R_d(kpc)$	3.5	3.5	3.5	3.5	3.5	3.
$R_c(kpc)$	5	5	5	5	5	15
ρ_\odot	0.008	0.008	0.008	0.003	0.007	0.005
β	-	-	0	0	0.2	0
q	-	-	1	1	1	1
V_a	-	-	165	100	170	170
$M_{Halo}(60kpc)(10^{11}M_\odot)$	5.1	5.1	1.9	0.7	1.2	2.2

Table 1: Parameters of power law model. First part of table represents the parameters of disk and the second part shows the halo parameters

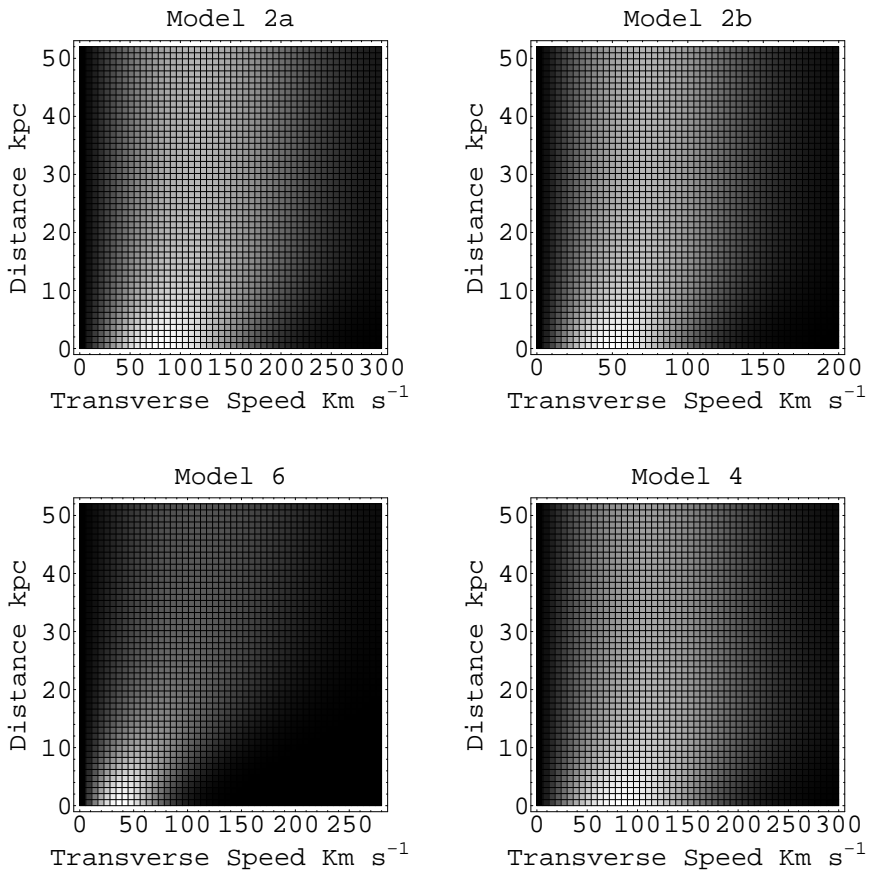


Figure 2: 2-Dimension histogram shows distribution of transverse velocity and distance of lenses from the observer located at the position of sun. Four panels are this distribution in Evans halo models 2a, 2b, 4 and 6.

4 Monte-Carlo Simulation

In this section we use Monte-Carlo simulation to obtain the theoretical distribution of events duration for each galactic models. We then apply the observational efficiency of EROS and MACHO groups to the theoretical distributions to obtain the expected distribution of events. One can compare these distributions with observed events and the aim is to put a constraint on the fraction of halo that can be made by Macho. Here, we supposed that all the microlensing events are due to halo or galactic disk lenses and we ignore those located in the LMC itself (self lensing). Next generation microlensing experiments with enough high sampling rate and better photometric precision, definitely will solve the question of self-lensing hypothesis [21].

As we mentioned before, three main elements for this Monte-Carlo simulating are the distribution of lenses, distribution of velocity and the mass function of Machos. For the mass function of the halo, we use the power law model as follows [22]:

$$P(M)d\left(\frac{M}{M_0}\right) = A\left(\frac{M}{M_0}\right)^\alpha d\left(\frac{M}{M_0}\right), \quad \text{for} \quad M_{min} \leq M \leq M_{max}, \quad (20)$$

where $M_0 = (M_{min}M_{max})^{1/2}$. The exponent $\alpha = -1.5$ according to the Expression (5) corresponds to an equal rate of microlensing events per decade of lens masses and also $\alpha = -2$ corresponds to an equal contribution to the optical depth per decade of less masses. In the range of $-1.5 < \alpha < -2$, the optical depth is dominated by massive objects and event rate is dominated by low mass objects. For the $\alpha < -2$ both optical depth and event rate are dominated by low massive objects, while for $\alpha > -1.5$ optical depth and event rate are dominated by massive objects. The domain for Mass Function is defined by β :

$$\beta = \log(M_{max}/M_{min}) \quad (21)$$

Here in this simulation we take $\alpha = -1.5$ and $\beta = 1$. One can simplify problem by identifying a mass scale. We assume such a mass scale is providing by a fixed upper mass limit, say $M_{max} = 1M_\odot$. The mass function of disk also is proposed by HST observation [25]. In the disk MF the slope is changed at $M \sim 0.6M_\odot$, from a near-Salpeter power-law index of $\alpha = -1.21$ to $\alpha = 0.44$. The best fit to mass function of disk indicated straight line, $d\log N/d\log M = -1.37 - 1.21 \log(\frac{M}{M_\odot})$ for $M > 0.6M_\odot$ and $d\log N/d\log M = -0.99 + 0.44 \log(\frac{M}{M_\odot})$ for $M < 0.6M_\odot$. Figure (3) shows the observed mass function by HST.

The spatial distribution of lenses in simulation along our line of sight is given by the equation (5) or in other word:

$$\text{probability of observation} \propto \rho(x)\sqrt{x(1-x)}$$

Using the galactic models mentioned in Table.(1), the distribution of lenses along our line of sight obtain according to Figures (4 & 5).

Here is the algorithm that we use it in our simulation:

In Monte-Carlo process we take the distance of the lenses from the observer according to its probability distribution via Figures.(4 & 5). The mass of the lens also obtain according to the corresponding mass function of Halo and disk models. We use the distance of lens form the observer and its mass to obtain corresponding Einstein radius of lens, by equation. (2). The transverse velocity distribution also

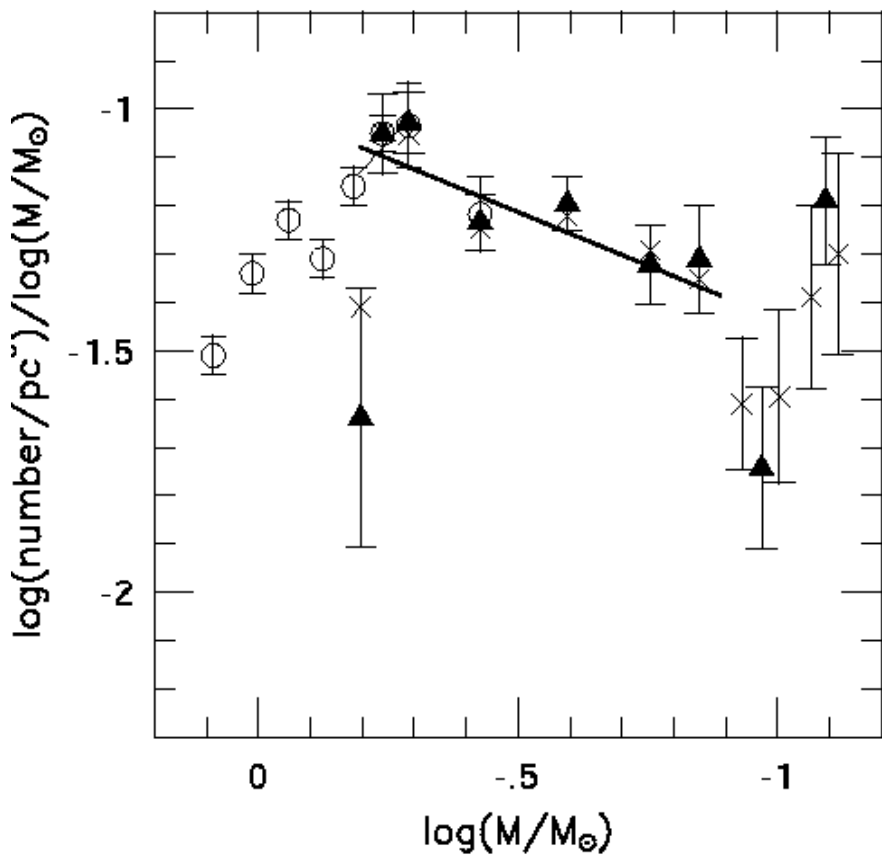


Figure 3: The mass function of disk [25]. The slope of the MF changes near the $M \sim 0.6M_{\odot}$, from a near-Salpeter power-law index of $\alpha = -1.21$ to $\alpha = 0.44$.

Distribution of Lens

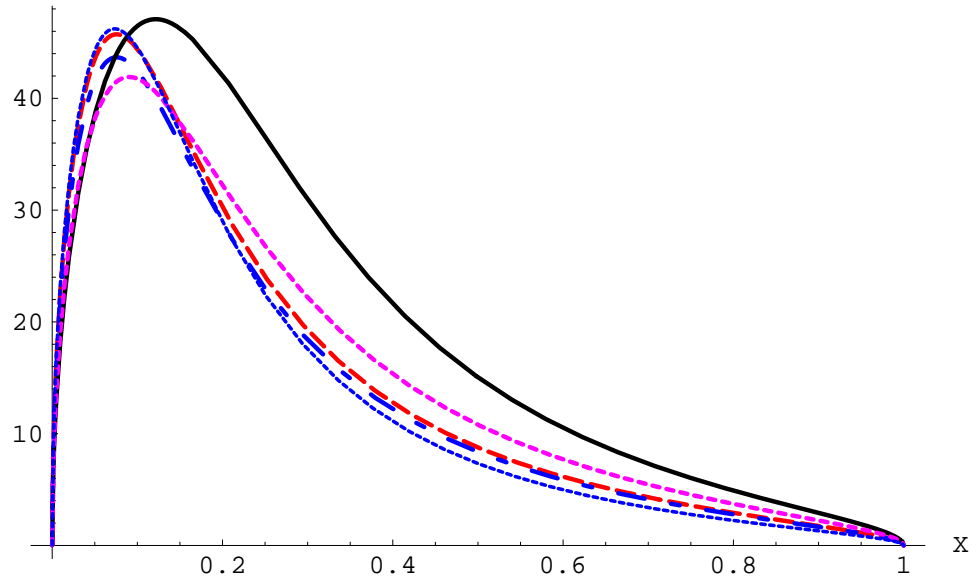


Figure 4: The distribution of lenses as function of distance from the observer in the different galactic halo models. dot-line stands for standard halo, dot-thin line for model 4, thick line for model 6, dot-dashed line for model 2b and dashed line represents model 2a.

Distribution of Lens

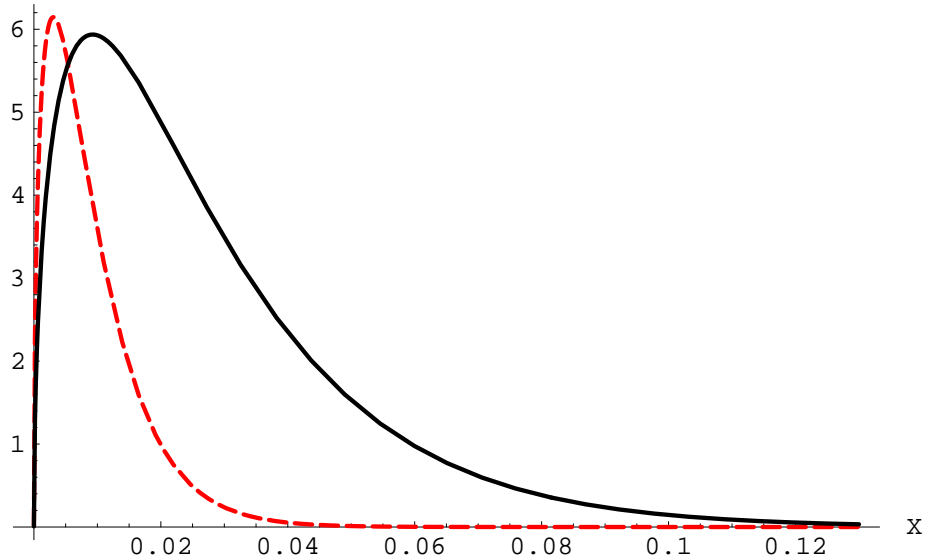


Figure 5: The distribution of lenses as function of distance from the observer in the different disk models. Solid-line represents this distribution in thick disk model and dashed line shows for thin disk model.

depending on desired galactic models obtain via Figures (1 & 2). One can combine the transverse velocities of lens from one hand and the Einstein radius from other hand to find the duration of events according to following formula:

$$t_E = 78.11 \left(\frac{M}{M_\odot} \right)^{1/2} \left(\frac{D_s}{10 \text{kpc}} x(1-x) \right)^{1/2} \left(\frac{200 \text{km/s}}{v_t} \right) \text{ days} \quad (22)$$

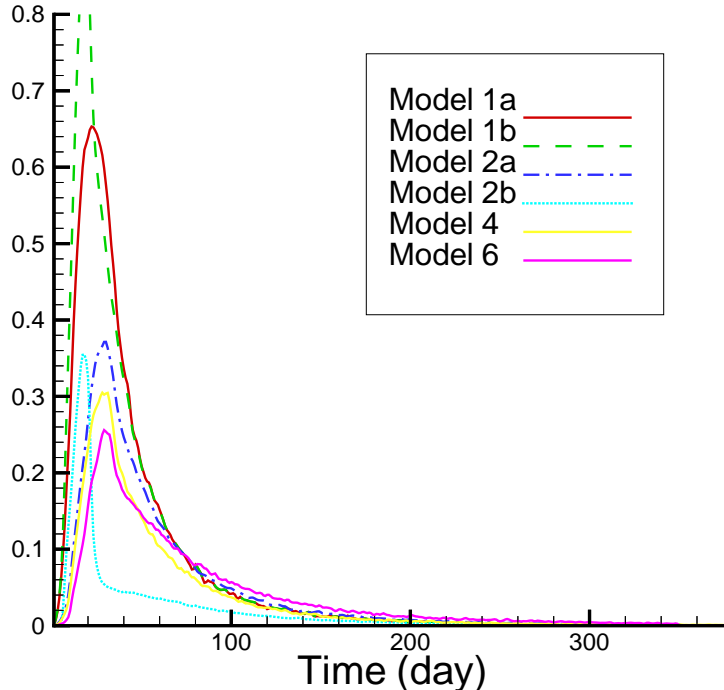


Figure 6: The distribution of events verses duration of events for different galactic models. The total number of events are normalized with the rate of events in one year for 10^7 background stars which obtained by Table 2.

Figure (6) shows the distribution of events for different galactic models, where the number of events are normalized $10^7 \text{star} \times \text{yr}$ exposure time with 100 percent efficiency in observation. The distribution functions are normalized to the total number of events (see equation (10)), using the numerical optical depth value and mean of inverse Einstein crossing time.¹ Table (2) as result of simulation shows corresponding optical depth and the rate of events in galactic models for $10^7 \text{star} \times \text{yr}$ exposure time. To obtain quantitative conclusion, we clearly need to assess our event detection efficiency. The detection probability for individual events is complication function of u_0 , t_E , the strategy of observation and the brightness of the source star. In fact all these distribution except t_E are not known and thus can be averaged over by a Monte-Carlo simulation. Here we use the observational efficiency of two experimental groups in our simulation. The detection efficiency for MACHO group which can be found in [23] and EROS group in [24]. For the efficiency calculation in EROS group, microlensing parameters are drawn uniformly

¹We used THalo code developed in EROS for optical depth calculation

Table 2: Optical depth and the rate of microlensing events is given toward LMC for each elements of galactic structure.

Model :	1a	1b	2a	2b	4	6
$\tau_{Halo}(LMC)10^{-7}$	4.96	4.96	3.92	1.44	2.82	3.58
$\tau_{Disk}(LMC)10^{-7}$	0.19	0.39	0.19	0.39	0.19	0.31
$\tau_{Total}(LMC)10^{-7}$	5.15	5.35	4.11	1.83	3.1	3.89
$\Gamma_{Halo}(/10^7 starYr)(LMC)$	41.5	41.5	18.21	5.53	16.38	15.
$\Gamma_{Disk}(/10^7 starYr)(LMC)$	2.20	4.40	2.20	4.40	2.20	3.52
$\Gamma_{Total}(/10^7 starYr)(LMC)$	43.69	45.89	20.41	9.93	18.58	18.52

in the following intervals: time of maximum magnification t_0 within the observing period ± 150 days, impact parameter normalized to Einstein radius $u_0 \in [0, 2]$ and time scale $t_E \in [5, 300]$ days [24], where the efficiency is normalized to events with an impact parameter $u_0 < 1$. The Efficiency of these two groups are shown in Figure. (7). It should be mentioned that the conventional definition of Einstein crossing time by EROS is the half of its value defined by MACHO group, here by convention we follow the time scale definition according to equation (22).

In what follows, we use the observational efficiency of gravitational microlensing detection in each experiments to obtain the expected number of events in different galactic models. Considering the whole matter of disk and halo is made by Macho we multiplying the efficiency distribution to the t_E distribution of model. It gives us the distribution of expected observation shown in Figure (8). Table (3) indicate overall expected number of events by EROS and MACHO for 10^7 time-object exposure in each galactic models.

The constraint on the contribution of dark compact objects to the galactic halo are obtained by comparing the number of microlensing candidates with those expected from Galactic halo models. Here we use two different statistical approach for analyzing EROS and MACHO data.

EROS group have been observed two candidate during 2 year observation of 17.5 million stars in LMC [26]. The observed microlensing events were called EROS-LMC-3 and 4 with Einstein crossing time in 41 and 106 days. Now, for statistical analysis, let b be the total expected number of events for a given galactic model (Table 3) and n_0 is the observed events in the absence of background. Considering the Poisson probability of observing events, one can obtain Poisson confidence intervals $[\mu_1, \mu_2]$ for n_0 observed events. In particular case we want to put an upper limit for b with a certain level of confidence. For instance, observing two event by EROS allows us to put a constraint, excluding (at 95% C.L) that the expected number of event can not be more than 6.72 or in another word, the expected number of events should be less than 6.72 with 95% C.L, let call this number C . Now, we normalize 6.72 to the number of events with $10^7 star \times yr$ exposure time to compare with Table. (3). The fraction of the halo made by Macho can be obtained by $f_M < C/F_M$ (at 95% C.L), where the F_M is the expected number of observation given in the Table. (3). The results for EROS in different galactic models indicated in Table (4).

The analysis of 5.7 year of photometry on 11.9 million star by MACHO group in the LMC also reveals 13-17 microlensing events [12]. We normalize the rate of events in Table (3) to the exposure time of MACHO group observation. For statistical analyzing of MACHO results, unlike the former exclusion approach that we used

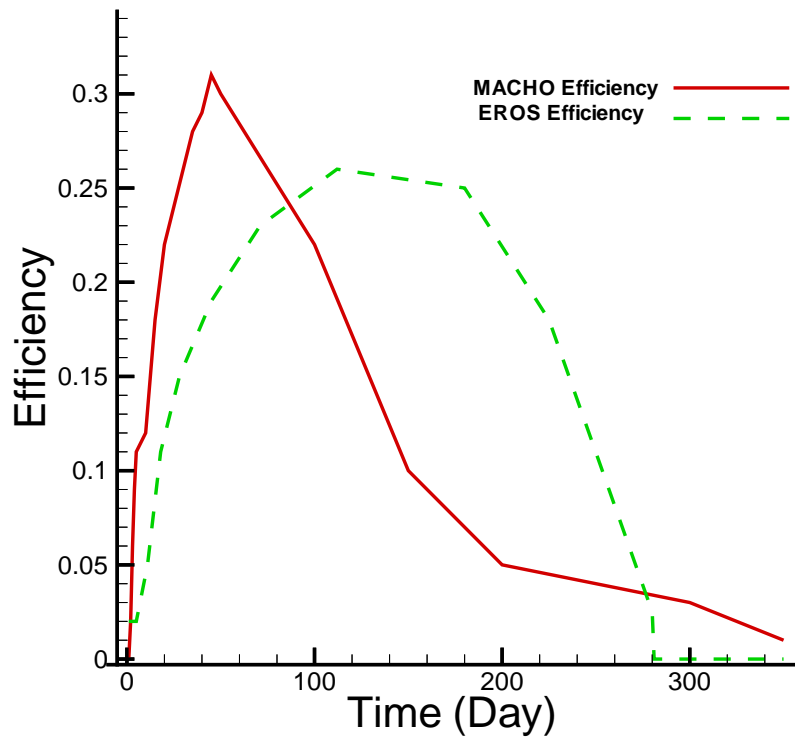


Figure 7: Detection efficiency versus event duration t_E toward LMC. The solid line shows the efficiency of MACHO [23] and dashed line indicate for EROS group [24].

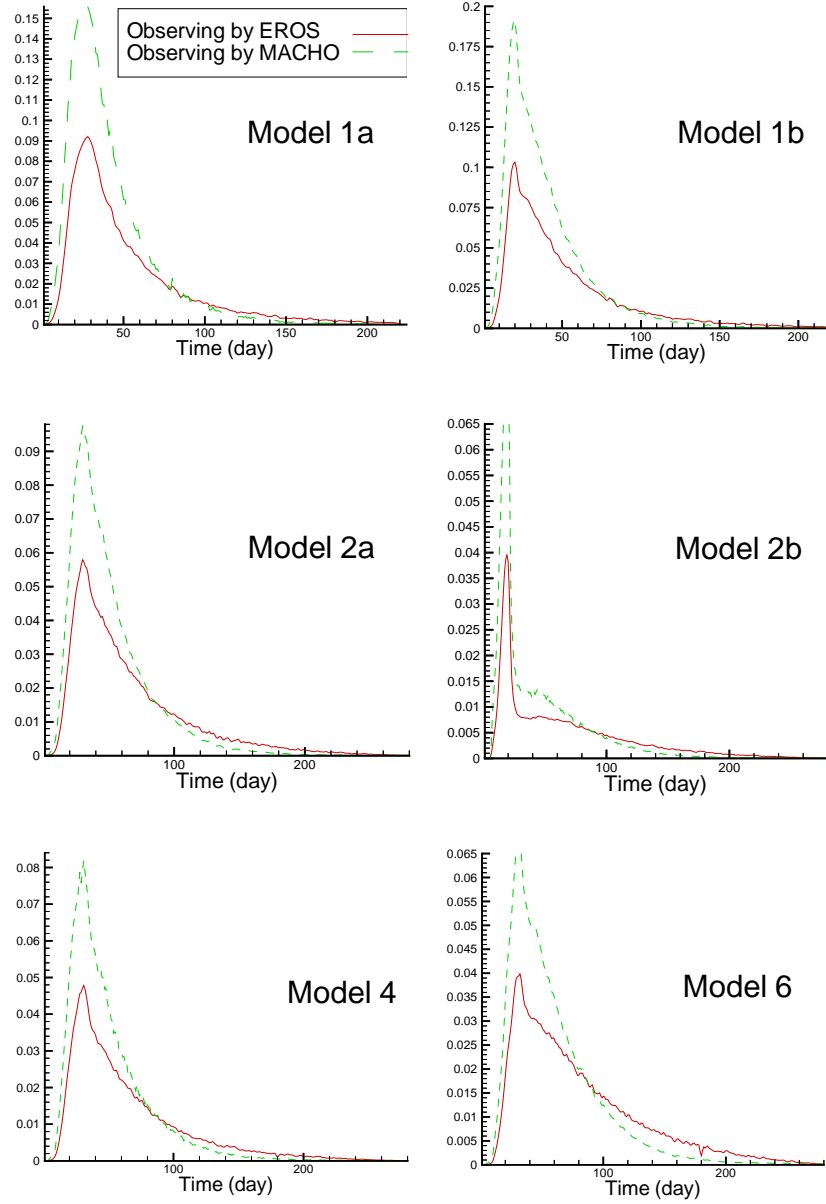


Figure 8: The distribution of events versus duration of events for different galactic models. The total number of events are normalized with the rate of events per 10^7 background stars in one year, Table 2.

Table 3: The expected number of microlensing events in $10^7 \text{star} \times \text{yr}$ exposure time for two experimental groups are obtained in six model.

Model :	1a	1b	2a	2b	4	6
EROS	6.81	6.93	3.64	1.59	3.29	3.23
MACHO	10.1	10.43	4.84	2.02	4.39	3.82

Table 4: The fraction of halo in the form of Macho obtain by comparing the observational results of two experimental groups with galactic models. This fraction depends on galactic model and the mass function of compact halo objects. The EROS results obtain by excluding with 95%*C.L* that this fraction should not be more than the indicated value. MACHO results also permit the indicated fraction of halo in the form of compact halo objects with one-sigma error.

Model :	1a	1b	2a	2b	4	6
$f_{EROS} <$	0.28	0.27	0.52	1.	0.58	0.59
f_{MACHO}	$0.25^{+0.06}_{-0.06}$	$0.24^{+0.05}_{-0.05}$	$0.52^{+0.12}_{-0.12}$	1	$0.57^{+0.14}_{-0.14}$	$0.66^{+0.16}_{-0.16}$

for EROS result, here we consider the part of halo mass that can be allowed to be in the form of Machos. The fraction of halo in the form of compact halo objects with one-sigma error indicated in Table. (4).

5 Conclusion

Considering two year of monitoring Large Magellanic Clouds by EROS and 5.7 year by MACHO, EROS detected 2 and MACHO 13 – 17 microlensing candidates. The results presented here provide some interesting conclusion on the contribution of Machos in the halo of our galaxy, depending on different Evans models. It is seen that except minimal halo model, the number of observed events are inadequate that halo fully comprised of $[0.1, 1]M_{\odot}$ compact halo objects. Two extreme results are considering a non spherical halo (minimal halo) for our galaxy or another possibility is an LMC halo that dominate microlensing, and no Machos in the Milky Way. Studying the exotic microlensing events like parallax effect, finite size effect and double lenses would allow us to locate precisely some lenses.

The fraction of halo (derived from microlensing experiments) in the form of Machos can also be compared with White dwarf [27] & [28] population studying in the Hubble Deep Field. Although the identification of these faint blue objects as white dwarfs remains to be confirmed and the small sample size restricts an accurate estimate, the suggestion that these White dwarfs could contribute 1/3 to 1/2 of the dark matter in the Milky Way. This result is in agreement with the fraction of halo in the form of Machos in some of halo models. The galactic halo, composed of White dwarfs would seem to be a natural explanation of the microlensing data.

References

- [1] Faber, S. M., Gallagher J. S., 1979, Ann. Rev. Astron. Astrophys 17, 135.
- [2] Trimble, V., 1987, Ann. Rev. Astron. Astrophys 25, 425.
- [3] Persic, M., Salucci, P and Stel, F., 1996, MNRAS 281, 27.
- [4] Moore, B., 1994, Nature 370, 629.
- [5] Navarro, J. F., Frenk, C. S., White, S. D., 1996, APJ 462, 563.
- [6] Copi, C. J., Schramm, D. N and Turner, M. S., 1995, Science 267, 192.
- [7] Burles, S., Tyler, D., 1998, APJ 499, 699.
- [8] Fukugita M., Hogan C. J., Peebles P. J. E., 1995, A&A 503, 518.
- [9] Paczyński B., 1986, APJ 304, 1.
- [10] Evans N. W., 19914, MNRAS 267, 333.
- [11] Spiro M., Lasserre T, *Cosmology and Particle Physics*, edited by Durrer, R., Garcia-Bellido, J and Shaposhnikov, M (American Intitute of Physics),(2001) 146.
- [12] Alcock C. et al. (MACHO),, 2000, APJ 542, 281.
- [13] Paczyński B., 1996, Annu. Rev. Astron. Astrophys 34, 419.
- [14] Roulet E., Mollerach S., 1997, Phys. Rep 279, 67.
- [15] Gould A, *A New Era of Microlensing Astrophysics*,edited by Menzies J. W., Sackett P. D., (ASP conference Series), preprint (astro-ph/0004042).
- [16] Jetzer P., 1997, Proceeding of 8th Marcel Grossmann Meeting on Relativistic Astrophysics, Jerusalem, preprint (astro-ph/9709212).
- [17] Binney S., Tremaine S *Galactic Dynamics*. Princeton University Press (1987).
- [18] Alcock C. et al. (MACHO), 1995, APJ 449, 28.
- [19] Renault C., PhD thesis, Université, Paris 7, DAPNIA/SPP 96-1003, (pub no. 96001264)
- [20] Palanque-Delabrouille, PhD thesis, University Paris 7 and University of Chicago, DAPNIA/SPP 97-1007
- [21] Rahvar S., Moniez M., Ansari R., Perdereau O., 2002 (submitted in A&A).
- [22] Mao S., Paczynski B., 1996, APJ 473, 57.
- [23] Sutherland W., 1999, Rev. Mod. Phys. 71, 421.
- [24] Palanque-Delabrouille N. et al. (EROS),, 1998, A&A 332, 1.
- [25] Gould A., Bahcall J. N., Flynnme C., 1997, APJ 482, 913.
- [26] Lasserre T. et al. (EROS),, 2000, A&A 355, 39.
- [27] Ibata, R. A. *et al.*, 1999, APJ 524, 1.
- [28] Meñdez, R. A and Minniti, D., 2000, APJ 529, 911.